

COMPARATIVE STUDY OF DIFFERENT FATIGUE CRACK GROWTH METHODS FOR THE DESIGN OF WIRE-WOUND VESSELS

J.M. Alegre¹, I.I. Cuesta¹, P.M. Bravo¹

¹ Structural Integrity Group. Escuela Politécnica Superior.
University of Burgos. C/Villadiego s/n, 09001. Burgos. Spain.
E-mail: jalegre@ubu.es

ABSTRACT

This work presents a comparative study of different fatigue crack growth methods for the assessment of wire-wound pressure vessels. The winding consist of a wire helically wound edge-by-edge in pretension in a number of turns and layers around the outside of an internal cylinder. The final result is a cylinder with compressive stress and the wire layers under tension. Under working pressure conditions, the vessel will be subjected to pressurization-depressurization cycles. According to the ASME code requirements, for the assessment of the vessel under cyclic loading an analysis of the fatigue crack growth must be performed. In general, three different approaches can be used: (a) Postulate a 1/3 semi-elliptical shape unchanged during crack growth, (b) Postulate a semi-elliptical shape that is updated at the deepest point and at the surface points, and (c) calculate by numerical analysis the crack front evolution during crack growth. The last approach will be obviously the most accurate, but the increase on the final number of cycles must be evaluated in order to justify the computational effort. This is one of the aims of this work. In addition, the procedure for the 3D crack growth simulation on the wire-wound vessels is widely explained in this paper. The effect of the mesh size in the computation of the stress intensity factor along the crack front has been analysed, and important recommendations for 3D crack simulations are provided. The strategy to update the crack front geometry during the crack growth process, useful for ANSYS users, is also provided.

KEY WORDS: fatigue design, wire-wound vessels, crack growth simulation.

1. INTRODUCTION

The wire-winding of high pressure vessels is a technique usually applied to introduce initial compressive stresses in the inner core of the vessel, with the aim to improve the fatigue life under cyclic pressure conditions [1-3].

Basically, the winding method consists of a wire helically wound edge-to-edge in pretension in a number of turns and layers around the outside of the inner cylinder. With each wound-wire layer becomes greater and greater compressive stresses in the cylinder, while the internal wire layers are slightly relieved as a consequence of the radial compressive stress generated by the last wound layer. The final winding process is a vessel with internal compressive stress in the inner cylinder and a wire winding block under tensile stress. Under working pressure conditions the initial compressive stress in the cylinder decreases and the winding tensile stress increases, but the internal core of the vessel can remain under compression if the initial compressive stresses are low enough. The compressive stress level that can be introduced in the vessel is obviously limited by the yield stress of the material under compression.

In order to calculate the number of design cycles based on crack propagation approaches it is necessary to define an initial crack size and an allowable final crack.

The initial crack size to be used for the calculation of the crack propagation design cycles shall be based on the nondestructive examination method to be used. In general, a semielliptical surface crack with a ratio of depth to surface length of 1/3 can be assumed. The allowable final crack depth must be calculated using the Failure Assessment Diagram (FAD) present on the Fitness For Service procedures (FFS).

In this work, three different levels of fatigue analysis are evaluated and discussed. First, a semi-elliptical crack shape unchanged during crack growth is postulated. This allows the tabulated solutions provided by the main design codes to be used. However, the natural tendency of the crack growth is not considered. Second, a semi-elliptical crack shape that is continuously updated, using the deepest and surface points, during the crack propagation is assumed. And finally, a finite element analysis to calculate step-by-step the crack front evolution during crack growth is analysed. This last approach will be obviously the most accurate, but the increase on the final number of cycles must be evaluated in order to justify the computational effort. This is one of the aims of this work.

In addition to this study, the numerical procedure for the 3D crack growth simulation on the wire-wound vessels is widely explained. The effect of the mesh size in the computation of the stress intensity factor along the crack front is discussed. The strategy for updating

the crack front geometry during the crack growth process, as well as important recommendations for 3D crack simulations, is provided.

2. GEOMETRY AND STRESS DISTRIBUTIONS FOR WIRE-WOUND VESSELS

In order to compare the approaches mentioned above and hypothetical vessel is considered in this study. The main dimensions of the cylinder and winding block are presented on Figure 1. An internal diameter of $D_i = 100 \text{ mm}$, an external diameter of the cylinder of $D_{if} = 200 \text{ mm}$, and an external diameter of the winding block of $D_o = 300 \text{ mm}$ are assumed. The vessel material is a high strength stainless steel with a yield limit of $\sigma_y = 1000 \text{ MPa}$. The pretension in wire is $S_w/\sigma_y = 0.8$ and the design pressure of the wire-wound vessel is $P_w = 5000 \text{ bar}$.

Analytical solutions can be found in literature to obtain the stress distributions generated by the winding process [1]. The radial and circumferential stress components, $\sigma_r(x_1)$ and $\sigma_t(x_1)$, for a cylinder coordinate x_1 , are defined by the following expressions:

$$\sigma_r(x_1) = - \left[1 - \left(\frac{D_i}{x_1} \right)^2 \right] \int_{D_{if}}^{D_w} \left(\frac{x}{x^2 - D_i^2} S_w(x) \right) dx \quad (1)$$

$$\sigma_t(x_1) = - \left[1 + \left(\frac{D_i}{x_1} \right)^2 \right] \int_{D_{if}}^{D_w} \left(\frac{x}{x^2 - D_i^2} S_w(x) \right) dx \quad (2)$$

where D_i is the inside diameter, D_{if} is the interface diameter between the winding and cylinder, D_w is the outside diameter of the actual winding layer.

Moreover, the corresponding stress in the winding diameter coordinate x_2 can be derived by:

$$\sigma_t(x_2) = S_w(x_2) - \left[1 + \left(\frac{D_i}{x_2} \right)^2 \right] \int_{x_2}^{D_w} \left(\frac{x}{x^2 - D_i^2} S_w(x) \right) dx \quad (3)$$

$$\sigma_r(x_2) = - \left[1 - \left(\frac{D_i}{x_2} \right)^2 \right] \int_{x_2}^{D_w} \left(\frac{x}{x^2 - D_i^2} S_w(x) \right) dx \quad (4)$$

Subsequently, the above equations can be easily integrated for a constant tensile stress value in wire during the winding process, $S_w(x)$, and they provide the stress distribution through the winding operation. Once the winding process has been concluded, the radial and circumferential stress components, both in the cylinder and the winding, can be obtained replacing D_w for D_o in the above expressions, where D_o

represents the outside diameter when the winding process is finished.

Figure 2 shows the circumferential stress distributions for the hypothetical vessel considered in this study, after the winding operation and under pressure conditions.

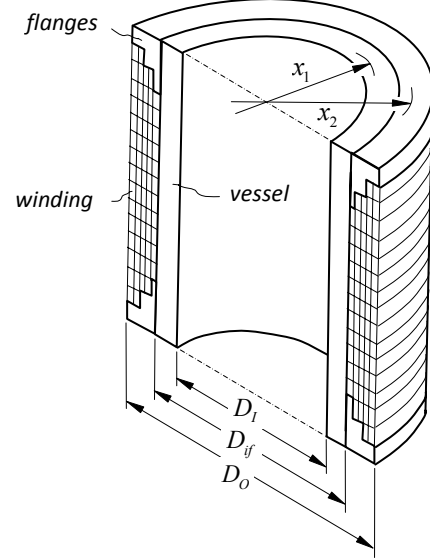


Figure 1. Nomenclature used for wire-wound vessels

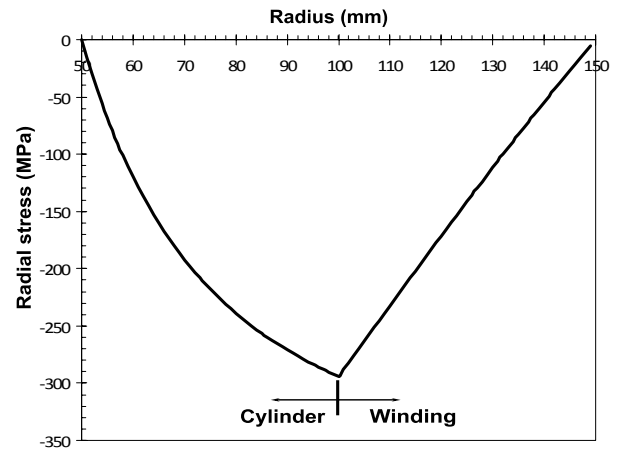
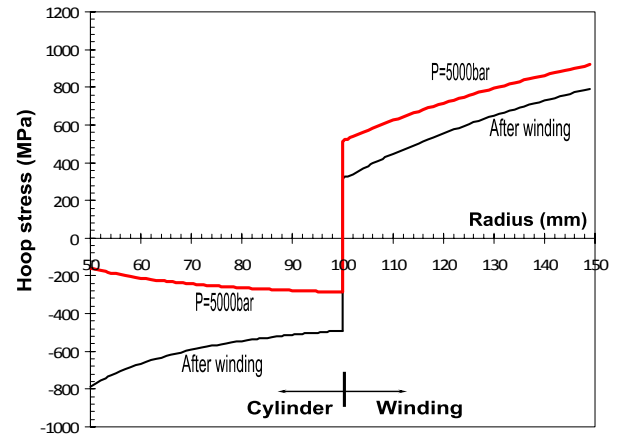


Figure 2. Radial and circumferential stress.

3. FATIGUE LIFE PROCEDURE

The first step for a fatigue life calculation is to consider an initial crack. In this paper, an internal crack in the longitudinal direction of the internal cylinder has been assumed, as is shown in Figure 3. A typical initial aspect ratio a_0 / ℓ_0 of $1/3$ and an initial crack depth of $a_0 = 0.2 \text{ mm}$ are postulated.

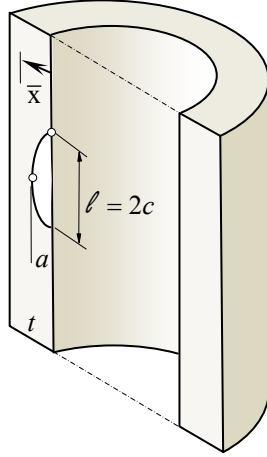


Figure 3. Semi-elliptical initial crack considered in the wire-wound pressure vessel

The next step consists on calculating the stress intensity factor range ΔK_I during crack propagation. Only the deepest point is considered for the first approach, both the deepest and surface points for the second approach, and all points along the crack front for the third approach.

According with the ASME code [1], the residual stresses introduced by the wire winding process have been considered separately by calculating an equivalent negative stress intensity factor $K_{I, \text{res}}$. The SIF by the internal pressure changes from a minimum stress intensity factor value of $K_{I(\text{min})} = 0$ when $P = 0$, to a maximum value of $K_{I(\text{max})}$ for the working pressure $P = P_w$.

As a consequence, a crack in the vessel without internal pressure has a stress intensity factor of $K_{I(\text{min})} + K_{I, \text{res}}$, and a crack in the vessel under internal pressure is subjected to an stress intensity factor of $K_{I(\text{max})} + K_{I, \text{res}}$. Then, the SIF range is:

$$\begin{aligned} \Delta K_I &= (K_{I(\text{max})} + K_{I, \text{res}}) - (K_{I(\text{min})} + K_{I, \text{res}}) = \\ &= K_{I(\text{max})} - K_{I(\text{min})} = K_{I(\text{max})} \end{aligned} \quad (5)$$

And the stress intensity ratio factor,

$$R = \frac{K_{I(\text{min})} + K_{I, \text{res}}}{K_{I(\text{max})} + K_{I, \text{res}}} \quad (6)$$

Note that the effect of the wire winding leads to a translation of the R -ratio towards negative values, without influence on the stress intensity range value.

Once the SIF range at the interest points is calculated, an incremental crack advance Δa for the deepest point is imposed (e.g. $\Delta a = 0.01 \text{ mm}$). The number of cycles ΔN_i needed to produce this crack advance is estimated using the propagation law as,

$$\Delta N_i = \frac{\Delta a}{C \cdot [f(R) \cdot \Delta K_I(a_0)]^m} \quad (7)$$

Where a propagation law that includes the effect of the R -ratio effect must be used, as

$$\frac{da}{dN} = C \cdot [f(R) \cdot \Delta K_I]^m \quad (8)$$

In this work the ASME code expression for R -ratio effect was considered [1], assuming material constants of $C(\text{mm/cycle}) = 5.29 \cdot 10^{-9}$ and $m = 3$ respectively.

The next step is to calculate the new crack size and shape for the next step. In general, the stress intensity range at any point of the crack front will be different. As a consequence, a different crack advance for each point is obtained after a block of cycles ΔN_i . At the deepest point the crack advance is the imposed value Δa , and the crack advance at other crack front point, Δc , is:

$$\Delta N_i = \frac{\Delta a}{C \cdot [f(R) \cdot \Delta K_I(a_0)]^m} = \frac{\Delta c}{C \cdot [f(R) \cdot \Delta K_I(c_0)]^m} \quad (9)$$

Where it can be easily derived that the crack advance at the surface is related with the imposed value at the deepest point, the stress intensity factor range for both positions, and the Paris law exponent m ,

$$\Delta c = \Delta a \cdot \left[\frac{\Delta K_I(c_0)}{\Delta K_I(a_0)} \right]^m \quad (10)$$

The procedure defined by the before steps is continuously repeated until the allowable final crack depth is reached. The number of cycles accumulated, from the initial crack to the allowable final crack, defines the fatigue life of the vessel. For the three approaches, the allowable final crack depth has been considered when the maximum SIF of the fatigue cycle reach a value of $K_{\text{mat}} = 150 \text{ MPa} \cdot \text{m}^{1/2}$. The maximum value of the SIF can be found at the deepest point or at the surface points of the crack, depending on the stress level of the vessel and the actual aspect ratio of the crack.

4. FATIGUE LIFE USING ANALYTICAL SOLUTIONS

An internal crack in the longitudinal direction of the vessel has been assumed in this study, as is presented in Figure 3. A typical initial aspect ratio of $a_0/\ell_0 = 1/3$, with an initial depth of $a_0 = 0.2\text{ mm}$, has been postulated. Other initial crack shape or sizes can be analyzed during the design stage of the vessel.

The first approach to obtain the fatigue life has been widely used over the past decades. It considers a semielliptical initial crack shape, and the stress intensity factor (SIF) is then calculated at the deepest point and used to define the next crack advance maintaining constant the aspect ratio of the crack. Its application is quiet direct, because nearly every one of the SIF solutions provided in the literature for semielliptical cracks is presented in tabulated form, as a function of the aspect flaw ratio.

The second approach can provide a more accurate fatigue life design, however the numerical procedure is more time-consuming because of the crack aspect ratio a/ℓ shall be updated as the crack size increases. The stress intensity factor, both at the deepest crack point and at the corner point, must be calculated in order to update the aspect ratio of the crack, assuming a semielliptical shape thought its fatigue propagation. This continuous crack shape updating requires tedious double interpolations if the conventional tabular solutions provided on the main design codes for SIF calculation are used [2]. Other closed-form equations can be used for this purpose [3].

For both approaches, the commonly method used to calculate the stress-intensity factor for internal semielliptical cracks in cylinders subjected to internal pressure (Figure 3) is based on the calculation of the stress distribution along the thickness, and then to fit it using a third-order polynomial equation as follows,

$$\sigma = A_0 + A_1 \cdot (\bar{x}/a) + A_2 \cdot (\bar{x}/a)^2 + A_3 \cdot (\bar{x}/a)^3 \quad (11)$$

Where A_0, A_1, A_2 y A_3 are the coefficients of the polynomial equation, a is the crack depth, and \bar{x} is the distance thought the wall measured from the flawed surface, as is shown in Figure 3.

If the distribution of stresses normal to the crack surface can be accurately represented by a single equation on the form of eq. (11) over the entire range of crack depths of interest, an alternate method can be used to compute K_I over this crack depth. The stress distribution can be obtained as:

$$\sigma = A'_0 + A'_1 \cdot (\bar{x}/t) + A'_2 \cdot (\bar{x}/t)^2 + A'_3 \cdot (\bar{x}/t)^3 \quad (12)$$

For each value of a/t the values of A'_i are converted to A_i values as,

$$\begin{aligned} A_0 &= A'_0 & ; & & A_1 &= A'_1 \cdot (a/t) \\ A_2 &= A'_2 \cdot (a/t)^2 & ; & & A_3 &= A'_3 \cdot (a/t)^3 \end{aligned} \quad (13)$$

The stress-intensity factor can be then calculated using the cubic polynomial stress relation given by eq. (11):

$$K_I = \sqrt{\frac{\pi a}{Q}} \cdot [G_0(A_0 + A_p) + G_1 A_1 a + G_2 A_2 a^2 + G_3 A_3 a^3] \quad (14)$$

where A_0, A_1, A_2, A_3 are the coefficients from eq. (11), A_p is the internal pressure of the vessel p that must be considered if the pressure can acts on the crack surfaces, G_0, G_1, G_2, G_3 are the free surface correction factors, and Q is the shape factor for an elliptical shape defined as,

$$Q = 1 + 1.493 \left(\frac{a}{c} \right)^{1.65} \quad \text{for } 0 \leq a/c \leq 1 \quad (15)$$

Each G_i has been obtained from the appropriate finite-element analysis by several authors, as Newman and Raju [2], and they are usually provided in tabulated form as a function of the crack shape, $a/2c$, and the crack size, a/t . These tabulated G_i -coefficients, or other similar, can be found in the pressure vessels design codes, as the ASME or API-ASME [3], or in usual literature [4]. In recent investigations analytical closed equations are provided, allowing the numerical integration of the propagation law to be more easily accomplished [3].

5. FATIGUE LIFE USING NUMERICAL SIMULATIONS

The last approach considered here uses the same postulated initial crack as the others approaches, but the crack shape is continuously updated along the fatigue crack growth process. In this sense, the SIF for all the points along the crack front must be determined. A consistent numerical procedure must be developed in order to carry out this approach.

The FE code ANSYS 10 [5] has been used for this numerical simulation. The mesh of the crack tip front has been constructed with 10 nodes singular elements, which have a quarter-node from the crack tip on the sides. A rate mesh transition of 1.5 has been considered from the crack tip to far from crack tip.

The displacement correlation technique (DCT) has been used for computing stress intensity factors in association with quarter-point elements [6-7].

The optimum value of the number of elements along the crack front was calibrated by comparison with analytical solutions. A reference geometry with a semi-elliptical crack was used. Figure 4 is shown two typical meshes for the crack line, and on Figure 5 is shown the effect of the number of elements on the crack front in the value for the calculated SIF. A mesh with 40 elements along the crack front, concentrated at the corner points has been selected as the most adequate.

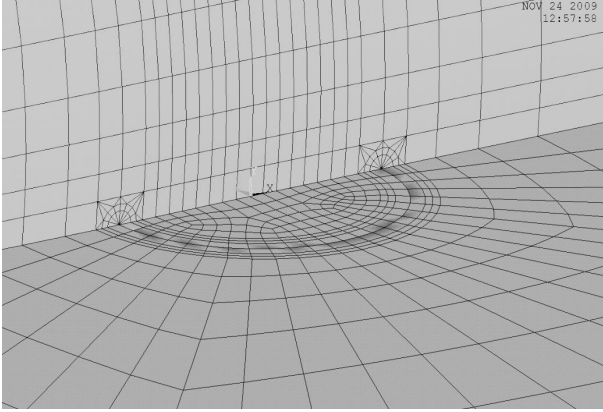


Figure 4. FE meshing used for crack growth simulation.

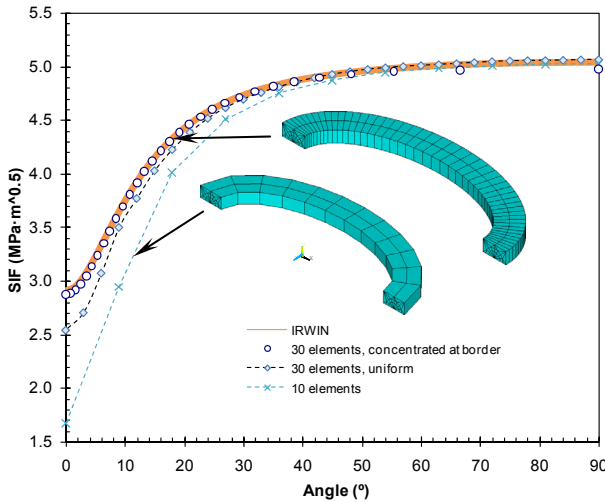


Figure 5. Effect of mesh on the SIF along the crack.

At each step, the fatigue crack growth has been estimated using the stress intensity range ΔK_I calculated for all points of the actual crack front and the propagation law of the material, according to the procedure explained on Paragraph 3. After a set of cycles, ΔN , the crack advance for each point of the crack front was obtained, and then a new crack front was defined to be used as the initial shape for the next step. This methodology allows the simulation, step by step, of the crack evolution from an initial crack to a final crack without assuming any standard shape during fatigue process. Figure 6 shows a simulation from an initial crack of $a_0 = 0.2\text{mm}$ and an initial crack shape of $a_0 / 2c_0 = 1/3$.

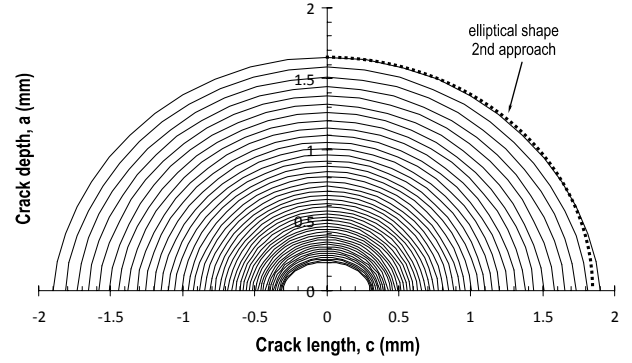


Figure 6. FE simulation of the fatigue crack growth.

In order to control the process the number of cycles for each step ΔN , is defined using the crack advance Δa_i corresponding to the maximal ΔK_I in the crack front.

Also, in order to achieve numerical convergence a great number of steps must be done due to the small coefficients of the propagation law, that it must be integrated using small steps in order to well obtain the number of cycles. For both reasons, as an example, if the initial crack size considered was 0.2 mm, a maximum crack advance of 0.01 mm has been used. After that, the crack advance was increased proportionally to the actual crack size $\Delta a_{i+1} = \Delta a_i + \Delta a_i / 20$. The maximum increase used was 0.1 mm in order to obtain a correct crack evolution for the longer cracks.

6. COMPARATIVE RESULTS

In the next figures are provided the comparative results for the three approaches considered in the present paper. For all the cases analysed, an initial crack depth of $a_0 = 0.2\text{mm}$ was considered, and the final crack depth is considered when the maximum stress intensity factor on the crack front reaches a value of $K_{mat} = 150\text{MPa}\sqrt{\text{m}}$.

Figure 7 presents the stress intensity factor evolution $K_{I(\max)}$, at the deepest point, for the three approaches. It can be observed that for the 1st approach the value of the critical SIF is reached when the crack extends up to 9.70mm, and the number of cycles to failure is estimated to be $N_f(1) = 91200$, as shows the Figure 8.

Figure 9 presents the crack shape evolution during the fatigue calculation using the 2nd approach and the FE simulation. It can be clearly observed that the crack shape grows up to a value of $a/2c = 0.45$. The number of cycles to failure using the 2nd approach was $N_f(2) = 128047$, and using FE simulation up to $N_f(3) = 124200$.

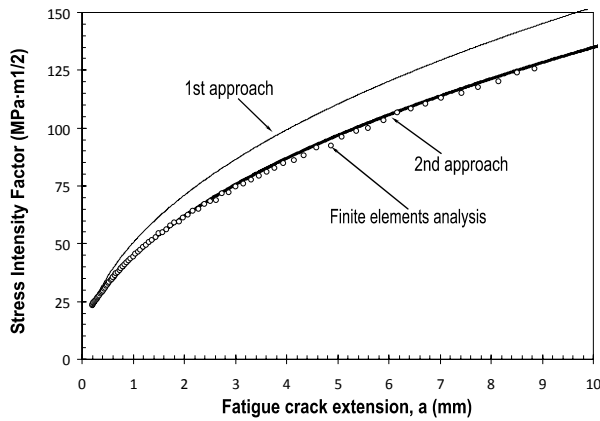


Figure 7. $K_{I(max)}$ at the deepest point

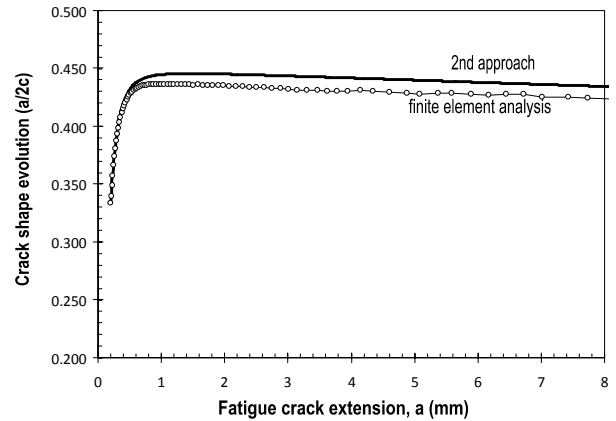


Figure 9. Crack shape evolution from $a_0 / 2c_0 = 1/3$.

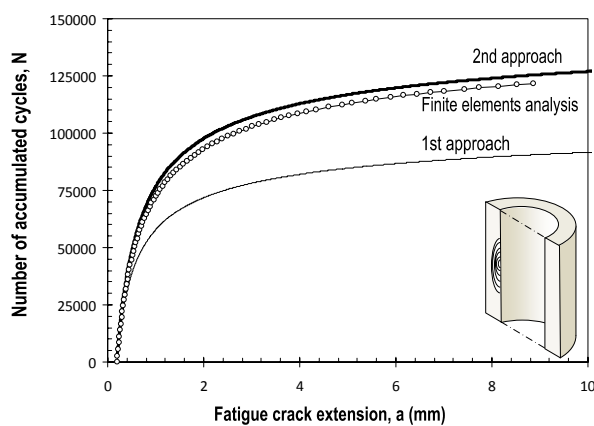


Figure 8. Number of accumulated cycles along the crack propagation, for the three approaches.

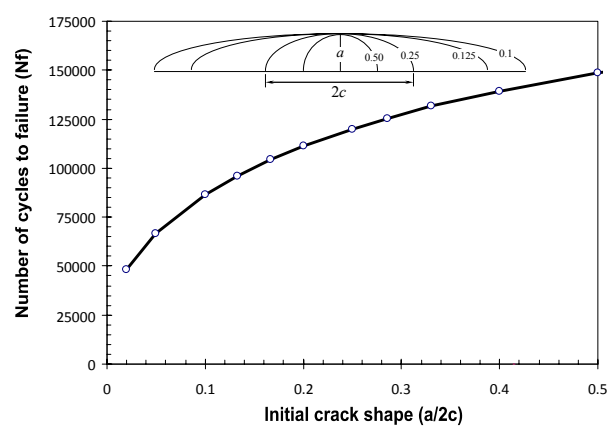


Figure 10. Effect of initial crack shape on the number of cycles to failure (2nd approach).

The initial crack shape considered has a relatively important effect on the fatigue life estimation. As an example, considering an initial crack shape of $a/2c = 0.45$ the number of estimated fatigue cycles using the 2nd approach reach a value of $N_f(2') = 139520$. The effect of the initial crack shape on the final fatigue life, using the 2nd approach is presented on Figure 10.

7. CONCLUSIONS

Three different approaches have been analysed to simulate the fatigue life of the wire-wound vessels. The results show that the first approach is not adequate to estimate the fatigue life, and a difference near the 50% can be obtained compared to the other approaches. The initial crack shape is also quite important in the number of cycles predicted. A tendency to $a/2c = 0.45$ is observed along the crack propagation, that results in a difference about 7% for the fatigue life respect to the initial assumption of $a_0 / 2c_0 = 1/3$. Finally, the difference between the numerical simulation and the 2nd approach is only 3%. In this case, the second approach provides a very good estimation of the fatigue life compared to a numerical simulation.

ACKNOWLEDGEMENTS

The authors acknowledge to JCyL research program (Project No.BU012A08) and NC-HYPERBARIC for sponsoring this research work.

REFERENCES

- [1] ASME (2007), *Alternative Rules for Construction of High Pressure Vessels in Boiler and Pressure Vessel Code, Section VIII, Division 3*. American Society of Mechanical Engineers.
- [2] ASME, *API 579-1/ASME FFS-1, in Fitness-For-Service*. (2007). American Society of Mechanical Engineers
- [3] Alegre JM, Bravo P.M., Cuesta I.I. (2009) Fatigue design of wire-wound pressure vessels using ASME-API 579 procedure. *Eng Fail Anal*, doi:10.1016/j.engfailanal.2009.08.008.
- [4] Newman J.C. and I.S. Raju, (1982) *Stress intensity factor for internal and external surface cracks in cylindrical vessels*. *J Press Vess Technol*. **104**: p. 293-298.
- [5] ANSYS 11 (2009). Finite elements code. User Manual.
- [6] Barsoum R.S. (1976) On the use of isoparametric finite elements in linear fracture mechanics, *Int. J. for Numerical Methods in Engineering* **10**, 25–37.
- [7] Bouchard P.O., Bay F., Chastel Y. (2003) Numerical modeling of crack propagation: automatic remeshing and comparison of different criteria. *Comput. Methods Appl. Mech. Engrg.* **192**, 3887-3908.